CLOSE: a self-regulating, best-performance tracker for modal integrator based AO loops

Vincent Deo, Milan Rozel, Arielle Bertrou-Cantou, Florian Moura Ferreira, Fabrice Vidal, Damien Gratadour, Arnaud Sevin, Yann Clénet, Gerard Rousset, Eric Gendron

CLOSE: a self-regulating, best-performance tracker for modal integrator based AO loops

V. Deo*, M. Rozel, A. Bertrou-Cantou, F. Ferreira, F. Vidal, D. Gratadour, A. Sevin, Y. Clénet, G. Rousset, and É. Gendron

LESIA, Observatoire de Paris, Université PSL, CNRS, Sorbonne Université, Université de Paris, 5 place Jules Janssen, 92190 Meudon, France

ABSTRACT

The pyramid wavefront sensor (PWFS), due to its extremely high sensitivity in comparison to the Shack-Hartmann WFS, is the design choice of most single-conjugate adaptive optics (AO) instruments currently being developed for extremely large telescopes (ELTs). This sensitivity benefit is served, however, with several technical drawbacks to overcome, one of which is the intrinsic non-linearity of the sensor. Even in modulated operation, the gradient measurement saturation non-linearity is strongly exacerbated by in-loop phase residuals for typical on-sky regimes, with high spatial frequencies inducing a dramatic sensitivity reduction for the controlled modes. This phenomenon has been dubbed "optical gain", and it was demonstrated that a modal gain compensation on an appropriate control basis provides an adequate mitigation of the sensitivity reduction, and improves the end-to-end performance on ELT SCAO systems across all relevant guide star magnitudes and seeing conditions.

Several techniques have been proposed to achieve this nominal performance recovery, however most require offline computation of interaction matrices; or some alterations to the usual AO loop operation. In this paper, we present the CLOSE (Correlation-Locked Optimization StratEgy) algorithm, which achieves determination of the modal gains, in a real-time fashion, through the sole use of the modal decomposition of the WFS measurements. Real-time estimators are implemented to implicitly measure resonance levels of the integrator transfer function, which is used as a proxy to control the modal gains through a second-layer servo loop. Using this method, we achieve compensation of the optical gain in the command law, and a fully automatic optimization of the modal integrator depending on the signal-to-noise level. Simulated end-to-end results are presented, for stationary or quickly varying seeing conditions, all at the scale of the MICADO SCAO design on the ELT. We also discuss the applicability of the CLOSE scheme on other known AO problems.

Keywords: Pyramid wavefront sensor, Extremely large telescopes, Modal control, Wavefront reconstruction.

1. INTRODUCTION

Probing the distant universe with always finer resolution and precision requires to increase the diameter of the next generation of ground-based telescopes[1–3] so as to improve light collection and resolving power. The latter is limited by atmospheric turbulence, making extremely large telescopes (ELTs) a waste if not for the use of adaptive optics (AO). The pyramid WFS[4] (PWFS) in particular is the preferred sensor for ELTs, a choice motivated by its increased sensitivity at low flux regimes, and also by technical advantages such as the reduced number of required pixels. Unfortunately, the PWFS also comes with a list of technical and theoretical difficulties and challenges; one such drawback is the variation of the sensor sensitivity with wavefront conditions,[5,6] called *optical gain*; sensitivity depends upon the magnitude and structure of the residual phase measured, and is thus influenced by the seeing, the wind speed or any other parameter that has an impact on the loop residuals.

Moreover, this optical gain intertwines with the integrator loop gain, i.e. the value used by the AO real-time computer (RTC) to scale the sensor feedback. Indeed, most AO systems use an integral controller, as such a law is conceptually simple and uses moderate computing power. Tuning the loop gain is a way to increase the loop performance, as gain impacts in opposite ways the temporal error and the noise propagation. A fine-tuned modal integrator thus makes it possible to optimally balance those error terms towards residual variance minimization.[7]

* Corresponding author. E-mail: vincent.deo at obspm dot fr

Previously existing approaches[7,8] are made complex by the sensitivity variation of the PWFS: the optical and loop gains multiply and bias the outcome: the sensitivity must be known to optimize the integrator.

We started to tackle this problem in the context of the SCAO module of the MICADO[9] instrument, a first-light, near-infrared imaging camera for the European ELT. The built-in SCAO[10] uses a PWFS working at optical wavelengths. We previously presented a method for estimating on-sky the optical gain,[11] and demonstrated that a modal compensation[12] applied on a well-suited basis allows for significant performance improvements, in particular for poor seeing conditions. Yet, we did not address the optimization of the integrator against the signal-to-noise ratio (SNR) and speed of turbulence, which is what we now propose in the present paper.

CLOSE (Correlation-Locking Optimization StratEgy) is a self-regulating method that permanently maintains the equilibrium between small temporal residuals and a reasonable noise amplification, while coping with an arbitrary hidden, variable WFS sensitivity, such as PWFS optical gain. Without assumptions, CLOSE applies beyond the sole case of the PWFS: it also naturally applies to any other AO system, whether the sensor gain varies or not (Shack-Hartmann systems, using or not quad-cells, elongated laser guide stars, etc). CLOSE – originally inspired by a proposition (Montera et al.[13]) to apply single-layer neural networks to AO RTCs– is a second-level servo-loop, which drives modal gains through real-time multiplicative updates computed from the temporal correlations of the modal decomposition of WFS measurements. The steady-state condition reached for this top-level loop closely matches the variance optimization criterion for the residuals, regardless of the currently-ongoing optical gain alteration of the WFS response. Altogether, CLOSE is a fully automatic, without intrusive signals, real-time pipeline optimizing integrator-based AOs with unknown sensitivity variations.

In section 2, we introduce our model of the PWFS and describe our dealing with nonlinearity. Section 3 explains how CLOSE operates, and section 4 will describe its possible implementations. Finally, section 5 shows some simulation results for the MICADO SCAO for stationary and varying seeing conditions, and discusses CLOSE capabilities beyond the originally envisioned PWFS modal gain compensation.

2. A QUASI-LINEAR MODEL OF THE NONLINEAR PWFS

We show on fig. 1 the schematic of the SCAO that is considered throughout this paper. The various wavefronts $\phi_\bullet$ represented on fig. 1 are meant as their vectorized decomposition on the control basis of the deformable mirror (DM): $(\phi_1, ..., \phi_N)$, plus some additional component orthogonal to the DM space. The wavefront sensor is represented by its modal interaction matrix **dPyr**, which is the differential of the WFS response, i.e. computed using infinitesimal push-pulls around a flat wavefront. We introduce before this interaction matrix a square, modal confusion matrix $\mathbf{M}$, which is a random variable dependent on the residual wavefront ϕ_{Res} shown to the PWFS. This random matrix $\mathbf{M}$ is the mathematical representation we choose of the optical gain effect.

The confusion matrix $\mathbf{M}$ has some reasonable properties when described on an appropriate modal basis, which are the foundation of optical gain modal compensation for the PWFS.[6,12] In previous work,[11,14,15] we performed a thorough numerical assessment of the fluctuations of $\mathbf{M}$ when the power spectrum density (PSD) of ϕ_{Res} is stationary, and validated the key properties described thereafter; these analyses were performed using

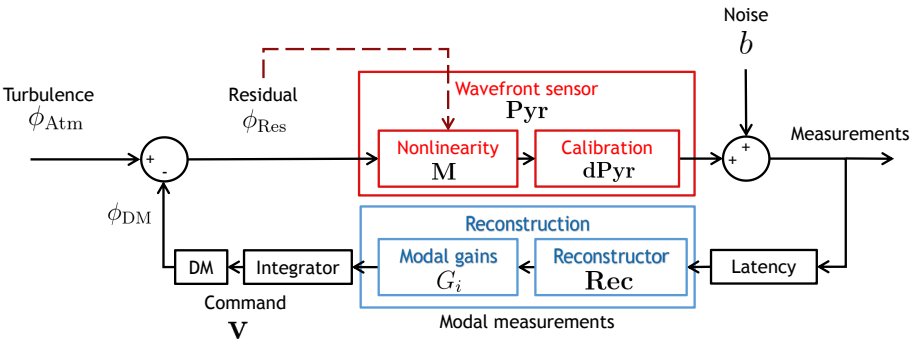

Figure 1. General modelization of the AO loop with the WFS, RTC and DM, in the nonlinear confusion matrix model presented. The confusion matrix $\mathbf{M}$ (slowly) depends on the structure of the residual ϕ_{Res}.

a Karhunen-Loève (KL) basis orthonormalized on the DM,[16] built with modes ϕ_i containing a mix of spatial frequencies of a single given norm, and ordered by spatial frequency. The last few hundred modes (at the ELT scale) contain a variety of waffles, until the cutoff is reached. We use this basis for all purposes in this paper.

We have demonstrated that: (1) $\mathbf{M}$ is essentially diagonal for low-order modes, which bear most of the power of the atmospheric turbulence; (2) that the diagonal coefficients vary by no more than a few percent for a given set of wavefronts ϕ_{Res} of identical PSD, a property in accordance with theoretical derivations through convolutional PWFS descriptions;[17,18] and (3) that the off-diagonal portion of $\mathbf{M}$, while non-negligible for high-order ϕ_i, is of a negligible average value across wavefronts of identical PSD.

These properties enable the modal gain compensation strategy. It is shown in the "Reconstruction" block of fig. 1: first, a modal space description is obtained through the reference command matrix $\mathbf{Rec} = \mathbf{dPyr}^{\dagger}$; then, an array of multipliers $G_{i,1\leq i\leq N}$ is applied to modal commands, with such multipliers ideally selected to encompass (1) compensation of the $\mathbf{M}$ nonlinear effect for ongoing turbulent conditions and (2) the gain factor such that the modal integrators show appropriate transfer functions and ideal rejection levels. The stability property of $\mathbf{M}$ against the spectrum of ϕ_{Res} ensures that G_i values can be kept constant as long as the descriptive statistical parameters (r_0, L_0, $C_n^2(h)$, ...) of the turbulence remain constant.

While we have well assessed that $\mathbf{M}$ is not, in general, a diagonal matrix, its average for a given ϕ_{Res} PSD is, and it remains quite interesting for design purposes to pursue this hypothesis in the general case. Assuming the diagonality, fig. 1 can then be simplified to the flowchart shown on fig. 2, which applies as one of N decoupled servo-loops for each of the controlled modes. The reference interaction and command matrices **dPyr** and **Rec** simplify to give scalar, decoupled diagrams, with $\mathbf{M}$ reduced to its $i-$th diagonal coefficient α_i. As α_i is always smaller than 1, it has often been called modal sensitivity *reduction*.

Under the diagonal hypothesis leading up to fig. 2, we can also factor in that α_i varies only with the statistical properties of the turbulence, and hence changes slowly relative to the rate the AO loop is executed at. Considering timescales over which all α_i are static, it follows that we simplified the problem of the nonlinear PWFS to N superimposed linear modal servo-loops, although each with an unknown sensitivity parameter. The performances of these loops are entirely defined by a small number of parameters: the temporal spectra of the turbulence and noise for the i-th mode, and the α_i and G_i scalars. The temporal spectrum for a single mode is well described in the literature[19,20] for Kolmogorov or Von-Kármán turbulence; we shall assume that the noise is white. The temporal dynamics of the loop are described by the sole "true gain" $\alpha_i G_i$, which effectively defines what the closed-loop transfer function will be. However, except for in-situ calibrations used by other optical gain compensation methods,[11,12,21] this overall loop gain is in general unknown to the operator and/or the RTC.

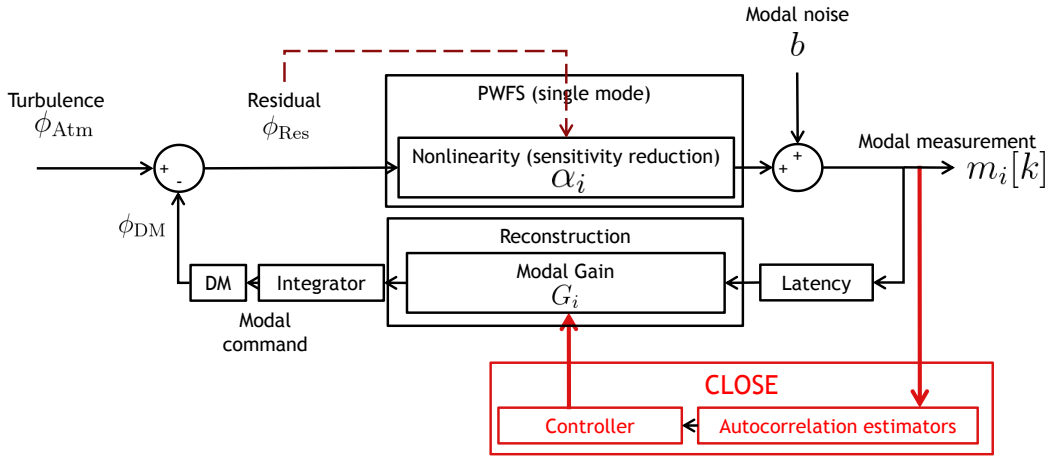

Figure 2. Reduction of the PWFS AO loop model (fig. 1) to a single mode. The matrix $\mathbf{M}$ is reduced to its i-th diagonal term α_i; residual off-diagonal terms are to be included in the modal noise b_i.

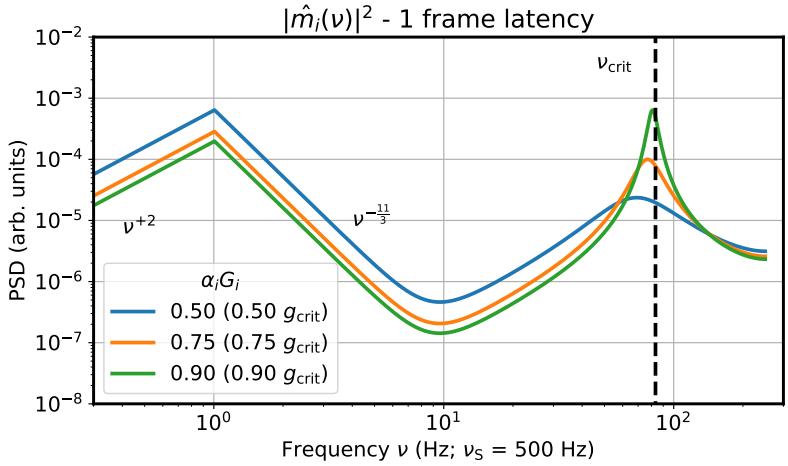

Figure 3. Typical temporal spectra $|\hat{m}_i(\nu)|^2$ of the residual closed-loop modal measurements for a high SNR case, for several values of the true gain $\alpha_i G_i$. Here the latency is 1.0 frame, $\nu_S = 500$ Hz, giving $g_{\text{crit}} = 1.0$ and ν_{crit}=83.3 Hz.

3. THE CLOSE SOLUTION TO MODAL GAIN

The diagram shown on fig. 2 introduces the principle of the CLOSE servo-loop; its objective is to provide a unified technique to optimize the rejection, defined by the hidden value $\alpha_i G_i$, based on the modal SNR, and operating only on the known modal multiplier G_i. It is introduced as a second-layer supervisory loop, which takes as inputs the modal decomposition of the PWFS measurements. From there, a frame-by-frame estimation of modal temporal autocorrelation (AC) is performed, and an update of the modal gain G_i is computed and applied at every time step based on these estimates. With all the priors on the temporal spectra of the modal components of the turbulence and noise, estimating the normalized AC for a single temporal shift enables the estimation of the actual loop gain $\alpha_i G_i$, and through this to automatically drive the value of G_i so that the transfer function given by $\alpha_i G_i$ is ideal for the control of the AO.

For each mode, the loop described in section 2 is a classical feedback loop with a delayed integrator of gain $\alpha_i G_i$. The rejection of such loops are a high-pass transfer function, and they become unstable when the gain reaches a value g_{crit}, which only depends on the loop latency (expressed in frame units). As the loop gain increases towards g_{crit}, the closed loop transfer function exhibits a typical resonance peak, with a central frequency converging towards a value ν_{crit} defined only by the system latency (expressed in frame units) as well. An example of modal measurements power spectra $|\hat{m}_i(\nu)|^2$, where ν is the temporal frequency and $\hat{\bullet}$ denotes a temporal Fourier transform, is shown on fig. 3. The left "peak" on fig. 3 is the remainder of the turbulence spectrum cutoff after application of the high-pass rejection transfer function. The right peak (converging to ν_{crit} – 83.3 Hz in this example with a sampling frequency ν_S of 500 Hz) is the result of the amplification of the noise floor as the AO loop, with an effective gain $\alpha_i G_i$ closing on g_{crit}, exhibits as strong resonant effect. The latency considered in the example shown on fig. 3 is 1.0 frame, resulting in $g_{\text{crit}} = 1$; in this paper, we define latency values as not including WFS integration and DM zero-order hold effects. Values of ν_{crit} and g_{crit} with latency are summarized in table 1.

Table 1. Parameters related to transfer function divergence of the AO loop depending on the latency of the system.

Latency (frames)	ν_{crit}	g_{crit}	Δt (frames)
0	ν_S / 2	2.0	1
1	ν_S / 6	1.0	3
2	ν_S / 10	≈ 0.618	5

The rationale of CLOSE is to leverage this typical structure of the modal measurement spectrum to implement a servo-loop supervising $\alpha_i G_i$. The amplitude of the resonant peak is used as a monotonically varying indicator to provide control on the value of the true gain $\alpha_i G_i$. The AO modal gain G_i is then adjusted to converge on the

desired $\alpha_i G_i$ value. In order to estimate the amplitude of the resonant peak, CLOSE uses the anti-correlation of the measurements for a time-shift Δt that is half the period corresponding to ν_{crit}. Values for Δt are also given in table 1. With $m_i^*[\Delta t]$ being the AC of the time series of modal measurements $m_i[k]$ for a time-shift of Δt frames, the normalized

$$\frac{m_i^*[\Delta t]}{m_i^*[0]} = \frac{\sum_k m_i[k] m_i[k+\Delta t]}{\sum_k m_i[k]^2}, \tag{1}$$

is a monotonic proxy for the true gain $\alpha_i G_i$. From there, one can act on G_i in order to lock the correlation value onto a steady-state solution verifying

$$\frac{m_i^*[\Delta t]}{m_i^*[0]} = r \in [-1, 1], \tag{2}$$

where r is the smartly chosen, supervisory loop setpoint. The value of r shall be adjusted (or defined per-mode) as to fit a performance-maximizing criterion in all useful situations the AO would face, and across the complete range of the effective modal SNR. A higher value for r will work towards a more cautious and robust solution with a lower loop gain. A smaller value will lead to more aggressive loop behavior, possibly reaching nearly-divergent transfer functions, but with a maximized rejection of the low frequency components.

With the condition of eq. 2 reached, CLOSE enforces a transfer function constraint that is independent of the sensitivity reduction of the WFS. Therefore, it provides a go-around strategy regarding the impossibility to apply to the PWFS (or other systems compatible with the description discussed in section 2) some methods[7,8] based on numerical estimations of transfer functions that are restricted to linear systems without unknowns.

3.1 Choosing the r setpoint

In order to assess what values of r shall be chosen, we performed semi-analytical computations of the steady-state solution of CLOSE, and compared to the optimal solution for modal integrators minimizing the residual variance of Gendron & Léna (1994).[7] As we use near-KL modes, the variance minimization is similarly obtained by optimizing each of the N modal loops separately.

These computations showed that for latencies of 0, 1 and 2 frames, and across 10 orders of magnitude of the range of modal SNR (i.e. for any mode and any SNR), the CLOSE steady-state solution never diverges from the optimal one by more than 20%, when keeping a constant setpoint value of $r = 0$. Certainly a smart fine tuning of the value of r could lead to some slight, marginal improvement of the performance. But we claim that choosing $r = 0$ is so close to the optimum over such a huge range of situations that it can be set as the baseline value with confidence. The retained value is not critical for the performance, provided it is not too close to -1 or +1. As said before, playing with values in $r \in [-0.2, 0.2]$ makes it possible to explore different compromises of performance versus robustness. These results show that CLOSE can, on top of making the loop independent from arbitrary hidden modal factors, enforce a near-optimization of the modal integrator with a very simple control law.

4. PRACTICAL IMPLEMENTATION

Having studied the steady-state solutions of the CLOSE servo-loop, we now propose our real-time implementation to achieve convergence to such states. From the time series $m_i[k]$ of modal measurements, two AC estimators are built using discrete integrators:

$$\begin{aligned} N_i^0[k] &= p\ m_i[k]^2 + (1-p) N_i^0[k-1] \\ N_i^{\Delta t}[k] &= p\ m_i[k] m_i[k-\Delta t] + (1-p) N_i^{\Delta t}[k-1], \end{aligned} \tag{3}$$

where k is the time step index, and $p \in [0, 1]$ a smoothing parameter. N_i^0 and $N_i^{\Delta t}$ contain time-windowed estimates of $m_i^*[0]$ and $m_i^*[\Delta t]$; after an empirical optimization of the parameter p, we opted for fast integrators with $p = 0.3$ for all simulations presented in section 5.

After the AC estimation, the G_i are updated using multiplicative increments as follows:

$$G_i[k] = G_i[k-1] \times \left[1 + q^{\pm}\left(\frac{N_i^{\Delta t}[k]}{N_i^0[k]} - r\right)\right]. \tag{4}$$

The r parameter is the same loop setpoint as defined in section 3. While the theoretical derivations were most accurate using $r = 0$, it is to be noted that for numerical simulations we maximized the long exposure Strehl ratio (SR) empirically, which in the end lead us to always using $r = -0.1$.

The $q^{\pm}$ learning factor encompasses two different values, with either q^+ and q^- used depending on the sign of $N_i^{\Delta t}[k]/N_i^0[k] - r$. This asymmetry is introduced as to make the algorithm more reactive to overshooting transients (with q^-), as compared to tracking gain increases due to a transfer function deemed too slow (using q^+). As such we will be using $q^- = 5q^+$; the numerical values of $q^{\pm}$ used in the numerical simulations in section. 5 are $q^+ = 10^{-2}$ and $q^- = 5.10^{-2}$.

These $q^{\pm}$ learning factors are the determining parameter of the time constants associated with the convergence and tracking ability of the CLOSE loop. Simulations here use what is near the maximum acceptable value to limit computation time while maintaining AO stability. We however infer that for a real AO system, q^+ values in the range of $10^{-3} - 10^{-4}$ should be used assuming 500 Hz frequency, hence providing typical time constants in the $2-20$ seconds range. The ideal choice of $q^{\pm}$ will probably remain dependent on the system, and will probably require some adjustments accounting for robustness and responsiveness to variations of turbulence conditions or other transient events.

4.1 Expected additional strain on the RTC

Implementing CLOSE in a real-time fashion is of course expected to add some additional RTC strain. While the AC estimations and gain updates themselves (eqs. 3 and 4) are negligible compared to the required matrix-vector multiplication (MVM), having the $m_i[k]$ available in real-time requires to do the reconstruction in two successive MVM steps. The first MVM converts WFS measurements to modal values, with a computational burden nearly identical to the usual measurements-to-DM-commands MVM. The second step computes DM increments from modal values, with a nearly square matrix of size the number of actuators.

For a typical PWFS AO system, the number of pixels read out is typically 5 to 6 times the number of actuators. If performing the measurement in a slopes-maps fashion, the RTC strain increase is of about 33 - 40%; if using a full-pixel measurement technique, it is an additional 16 - 20% increase only.

4.2 Block-wise, zero-strain alternative

If the RTC software cannot be altered on an existing system, or if the additional strain is not acceptable within the RTC specifications, CLOSE can be implemented in a block-wise flavor. In such case, all estimators, gain updates, and command matrix updates are performed in offline time, certainly in another process and preferably on another machine. This buffered strategy enables to deploy CLOSE on nearly any existing AO system.

A time-continuous buffer of K WFS measurements is forwarded to the CLOSE process, which turns them into modal measurements $m_i[0]...m_i[K-1]$ using the modal reconstructor **Rec**. For each mode, the AC estimators of eq. 3 are replaced by the direct computation of the normalized Δt-shifted AC term over the telemetry buffer:

$$N_i^{\text{block}} = \frac{\frac{1}{K-\Delta t}\sum_{k=0}^{K-\Delta t-1} m_i[k]m_i[k+\Delta t]}{\frac{1}{K}\sum_{k=0}^{K-1} m_i[k]^2} \tag{5}$$

The gain update equation can then be performed:

$$G_i[\text{new}] = G_i[\text{old}] \times \left[1 + q^{\pm}\left(N_i^{\text{block}} - r\right)\right], \tag{6}$$

using $q^{\pm}$ factors adjusted for the longer integration time and the increased SNR on AC estimation; typically $q^{\pm}$ ought to be larger by a factor $\sqrt{K}$ for a dynamical effect comparable to the real-time implementation. The new command matrix can then be computed accounting for the new G_i values, and when all side-tracked computations are finished, can be set into the RTC.

5. NUMERICAL SIMULATION RESULTS

This section covers some end-to-end numerical simulations demonstrating the performance achieved with CLOSE when applied to the MICADO SCAO design[10,22] (see table 2). All simulations were performed using the COMPASS[23] platform. In the following sections, we present studies on the convergence of modal gains when bootstrapping the AO loop, and the end-to-end performance for stationary and varying seeing conditions. In addition, videos showing the dynamical behavior of some CLOSE simulations are available online.[24]

5.1 Gain convergence at loop closing

We can take a first look at the behavior of CLOSE when the AO loop is closed. Without any priors given, we choose an initialization condition $G_i[0] = 0.5$. With the 2 frames of latency considered, the critical gain value is $g_{\text{crit}} \approx 0.61$; given that the sensitivity reduction α_i is always smaller than 1, this ensures that the loop is initially closed with stable transfer functions. From these initial 0.5 values, the G_i are driven by CLOSE to their steady-state values, which account both for non-linearity compensation and the temporal variance minimization.

We show on fig. 4 the values of the 4 309 modal gains G_i, averaged on certain subsets of frames within the first two seconds after the AO loop is closed. These simulations are performed for four different cases, with r_0 of 14.5 and 9.0 cm, and guide stars of brightnesses $M_R = 0$ and $M_R = 16$. For the bright cases, steady state is reached by frame $k \approx 500$, i.e. within one second. The process is slightly slower for the $M_R = 16$ cases, with a continued convergence of the G_i between frames $k = 500$ and $k = 1000$.

Simulations at $M_R = 0$ are essentially performed with an infinite SNR. As such, the loop true gain which minimizes the output variance is close to the maximum stability value g_{crit}, and the G_i coefficients reached in steady-state are essentially reflecting the inverse α_i^{-1} of the PWFS sensitivity reduction. These curves reached after $k = 1000$ frames in $M_R = 0$ cases are compliant with the abacuses we presented in previous work,[11,14] with α_i decreasing up to mode 30, which contains spatial frequencies corresponding to the modulation radius, then increasing again roughly as a power law up to the highest order modes.

Table 2. AO parameters used for end-to-end numerical simulations

Simulation parameters

Telescope	D = 39 m	**Turbulence**	von Kármán - single ground layer
	ELT pupil model		r_0(500 nm) from 7.0 to 22.0 cm
	Spiders are omitted		$L_0 = 25$ m, $\|\|\vec{\mathbf{v}}\|\| = 10$ m.s^{-1}
Guide star	On-axis natural star	**PWFS**	92×92 subapertures (42 cm pitch)
	zero point 2.6×10^{10} ph.s^{-1}.m^{-2}		24 080 pixel values read-out
DMs	Tip-tilt		"Full pixels" measurement space[25–27]
	ELT M4 model		Monochromatic at 658 nm
	pitch 54 cm, coupling 0.24		0.28 throughput (quantum efficiency inc.)
	4310 actuators driven		Circular modulation, $r_{\text{Mod}} = 4\frac{\lambda}{D}$
RTC	Frequency 500 Hz		Read-out noise 0.3 e^-
	Latency 2 frames	**CLOSE**	Real-time implementation
	(exposure/hold **excluded**)		$p = 0.3$
	Controlled on KL basis[16]		$q^+ = 10^{-2}$, $q^- = 5.10^{-2}$
	Modal integrator with double MVM:		$r = -0.1$
	Pixels $\longrightarrow [m_i] \times [G_i] \longrightarrow$ actuators		

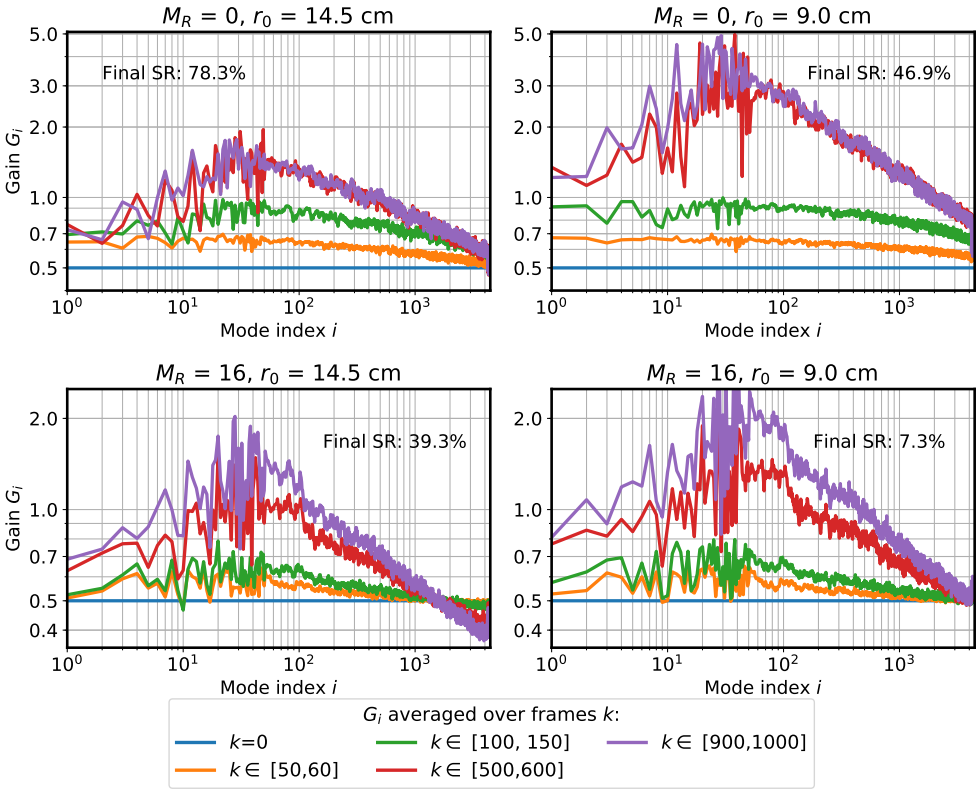

Figure 4. Convergence of CLOSE gains on the 2.0 sec following loop closing, for guide stars of $M_R = 0$ and 16 and atmospheric r_0 of 14.5 and 9.0 cm. All G_i are set to 0.5 at loop closing (blue line). G_i values are shown as averaged over the frame intervals given in the legend. Curves are smoothed along the i index for clarity. Final SRs are given in H-band and computed from the cumulative exposure between frame 900 and 1000 (200 msec).

When comparing the G_i values reached between $M_R = 0$ and $M_R = 16$ cases, one can observe the effect of the SNR-dependent optimization of the transfer function, with steady-state gain values dampened by typically 20-50% depending on the mode number and the r_0. Altogether, results presented on fig. 4 tend to validate that – without any priors and regardless of the PWFS sensitivity reduction – CLOSE is able to make the modal integrator adaptively converge to the adequate solutions, across a 1 to 2 second period.

5.2 Results with stationary turbulence

Besides the adaptive capability, it is most important to look at the AO performance achieved once CLOSE reaches its steady-state behavior. In order to perform this analysis, we generalize the simulations to a larger range of r_0 values and guide star magnitudes.

Measured performances are shown on figure 5, with the long exposure H-band SR plotted against the star magnitude and computed for 5 different seeing conditions. For all the results the SR is averaged over 2-second exposures, starting 2 seconds after the AO loop is closed, and with initial modal gains $G_i = 0.5$ as previously.

We report the performance achieved for r_0 values from 8.9 to 21.5 cm, and for guides stars from $M_R = 10$ to 17.5 with CLOSE (**solid lines**). **Circles** overlaid at $M_R = 10$ and 16 are performance without using modal gain compensation, but after an optimization of a global scalar loop gain. **Square markers** are when using the dithering-based determination of modal gains as reported in previous work,[11] and after an optimization of the scalar loop gain. The latter dithering-based performance is also identical to what can be obtained using the sensitivity normalization, the original method proposed by Korkiakoski *et al.*[6,12]

From the performances reported, it follows that CLOSE compares to other modal non-linearity compensation techniques crafted for high-order PWFS, with added benefits: a single, real-time technique factors in both the

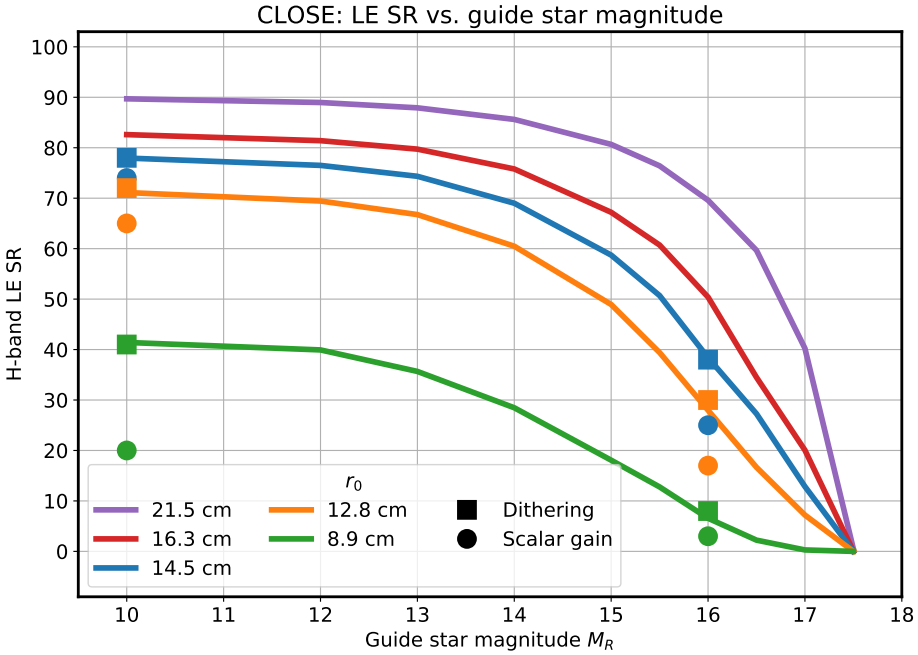

Figure 5. Plain lines: Long-exposure SR in H-band obtained with CLOSE for guide star magnitudes M_R=10 – 17.5 and r_0=8.9 – 21.5 cm. Circles: Best performance obtained without using modal gains. Squares: Best performance with modal gains optimized through a dithering measurement technique, recalled from previous work.[11]

non-linearity component and the transfer function optimization, with a far greater responsiveness to transient events; and as compared to either of the aforementioned modal compensation techniques, offline computation of modal gain abacuses or in-situ control matrices is no longer required.

5.3 Continuously varying turbulence

When mentioning the robustness of CLOSE regarding optimizing the modal integrator through transient events, it is interesting to evaluate how the performance evolves for continuously varying seeing conditions.

We report on fig. 6 the results of a simulation in which the r_0 value changes from 22 cm to 7.0 cm then back to 22 cm over the course of 100 seconds of operation, without ever opening the AO loop or performing any external action on the AO parameters. A similar simulation was performed in previous work[11] for several gain compensation strategies. The performance is measured in terms of SR over successive 0.1 sec (solid lines) and 2 sec exposures (circles), starting 2 sec. after the loop is closed. An identical experiment is ran for guide stars of $M_R = 5$ and $M_R = 16$.

In practice, the COMPASS-generated numeric turbulence screen is continuously extruded from one edge of the pupil, then translated with the simulated wind. The r_0 given on fig. 6 is the one of the wavefront pixels being extruded at a given time; yet it takes 4 seconds for those turbulent features to entirely cross the pupil. This induces a delay of about 2 seconds between the time a given r_0 is reported, and when the associated performance is expected on the imager.

The SR complies with the values found for stationary r_0 cases for the bright and the $M_R = 16$ case, demonstrating that although the seeing conditions vary very quickly, the responsiveness of the modal gain curve can easily adjust the integrator regime for such variations, maintaining the maximum possible SR for a given r_0/M_R combination. The symmetry of the two r_0 decreasing and r_0 increasing phases is also to be noted: CLOSE enables the integrator to accommodate both cases with similar flexibility. Cases with the seeing improving were noticeably less robust with previous modal compensation methods, as the increased sensitivity of the PWFS can lead to a diverging integrator if the modal gains are not adjusted in a timely manner.

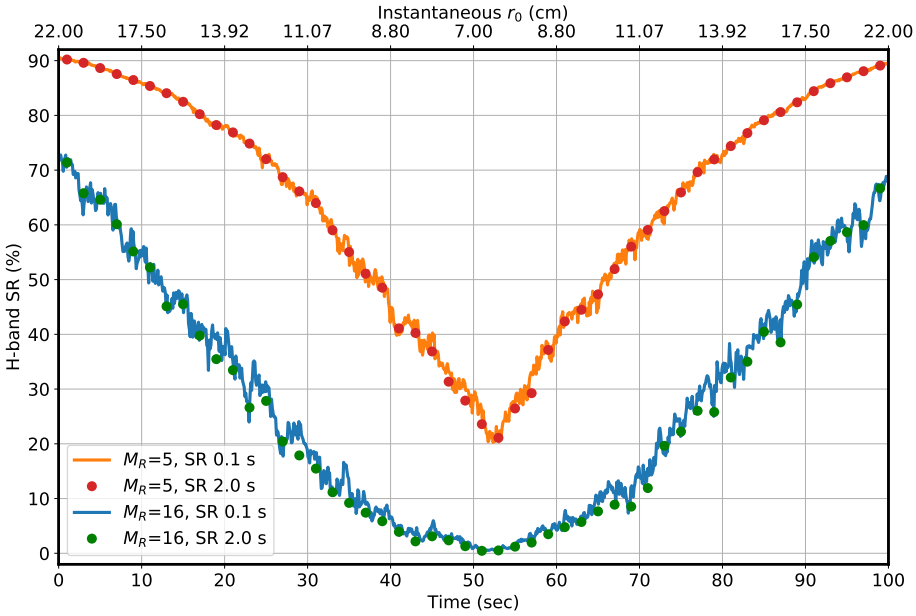

Figure 6. SR in H-band obtained for 0^{th} and 16^{th} guide star magnitudes, as the seeing conditions cycles from $r_0 = 22$ cm to 7 cm and back across 100 sec of simulated AO time. Lines: 100 msec SR; markers: 2.0 sec SR.

The symmetry, in particular at $M_R = 16$, also underlines that the integrator is adequately maintained in a robust regime, without accumulation of waffle or divergence of single actuators, after more than 20 seconds spent with a residual wavefront error of about 1 λ RMS on the PWFS.

5.4 Additional capabilities

Not only CLOSE is able to track gains through varying observing conditions[24a], but it can also adapt the system to some other situations. We have simulated CLOSE when sensing on double stars[24b], and tested the results against different separations, different orientations with respect to the pyramid edges, and different flux ratios of the guiding binary. The detailed results have not been reported in this paper, but we were able to verify that the functioning point reproduced the same performance that could be obtained using standard methods. This also demonstrates that an interaction matrix for a single star can be converted to another adequate to binary sources using a modal rescaling only on our DM KL basis.

The test has also been done using uniform disk-like objects of various diameters from 10 to 800 mas (a simulation of Titan as guide object[24c]). Not surprisingly, each of them exhibits a similar behavior where the gains stabilize rapidly to the optimum value, with a performance level consistent with that found using classical methods. The case of more peculiar objects (triple or multiple stars, galactic nuclei exhibiting a plateau around a central peak, small globular clusters, etc.) has not been studied but we are confident that CLOSE would also converge smoothly on those cases.

Also not tested yet when writing the present article, we think that CLOSE can also cope with variations of the modulation radius (without a substitution of the command matrix), as this impacts the WFS sensitivity –at first order– as a modification of the modal gains. Whether that interesting property can be leveraged is another, wider topic to be discussed in the perspective of optimizing the overall pyramid sensor behavior even better.

We also need to mention that CLOSE can be applied to systems using other wavefront sensors than pyramids. In particular, CLOSE could certainly help in the case of the *centroid gain* induced by quad-cells in a Shack-Hartmann sensor, which acts as a global unknown multiplicative factor. We think it could also be of some help in the case of significantly elongated laser guide stars (LGS), possibly truncated, which induce some unknown fluctuations of the sensitivity in the measurements with the thickness changes of the sodium layer. However, we think this would possibly have to be coupled with a smart choice of the modal basis to act on. We envision a scheme where one CLOSE loop is run in the slope space to compensate centroid gain effects, and another in the

modal space for integrator optimization, held together with adequate normalization conditions. We think that CLOSE could be of help any time a modal gain optimization on an integrator law is to be done in a situation where sensitivity fluctuations (either of the sensor, or the adaptive mirrors) are to be expected.

CONCLUSION AND PERSPECTIVES

We have presented a self-regulating method that allows us to track, either in hard or soft real-time, the modal gains of the integrator controller in an AO system, in order to maintain the maximum performance against variable conditions (seeing, wind speed, SNR) and variable sensitivity of the WFS. Our method differs from previous works as it doesn't require any knowledge about the sensitivity of the sensor, but permits to counteract its variations. This property makes the method particularly suitable whenever sensitivity fluctuations of the feedback loop (either of the sensor, or the adaptive mirrors) are to be expected, like in the case of high-order PWFS designs on ELTs.

The method is based on the value of the temporal auto-correlation of the modal phase residuals computed at a single given time-shift Δt, followed by the appropriate counter-reaction on the modal gain in order to lock the previously mentioned Δt-*correlation* value to some chosen setpoint. We have demonstrated first that, for some given conditions, there is an unequivocal relation between the gain and the value of that Δt-correlation, and second that locking the Δt-correlation at a fixed well-chosen value through multiplicative adjustments of the integrator gain will keep the phase residuals near their achievable minimum. The method has been called *CLOSE*, for Correlation-Locked Optimization StratEgy.

We were able to experience through end-to-end AO simulations the remarkable behavior of the CLOSE algorithm: extremely promising, it appears to be self-regulating, and seems to adapts naturally to any new case whether we deal with any combination of good or low SNR, good or bad seeings, extended objects or else.[24] However, our simulations at the time of writing are restricted to a PWFS (that of the SCAO module of MICADO ELT instrument, which was the primary target for our study). We are confident that CLOSE also applies to others AO systems equipped with non-pyramid sensors: future numerical simulations should be able to confirm this, and there is certainly a wealth of potential applications to follow. Today, CLOSE is our baseline algorithm for optimizing the end-to-end simulations running with a pyramid sensor.

Coming now to limitations, we shall warn potential users that the update equation (eq. 4) contains an integrator, which definitely requires a proper feedback to avoid any fatal divergence. Blocking of the feedback on the correlation value may be triggered by unexpected effects, such as actuator saturation on the deformable mirror, or by the absence of feedback from the main AO loop –which happens when the loop "crashes" or when the flux disappears. Other cases may exist, but those are sufficient to draw our attention to the fact that eq. 4 needs to be completed with some monitoring and safeguarding system in order to be fully applicable to a real system. We shall also investigate the impact of non-Kolmogorov input perturbations such as telescope wind-shake, or vibrations. While telescope wind-shake is generally a low-frequency perturbation that should not harm too much the algorithm, the way CLOSE will interact with high-frequencies vibrations potentially amplified by the rejection overshoot remains to be looked in detail. Whether CLOSE reacts in a right or wrong way depending on the frequency of the perturbation is not obvious at first sight.

Finally, it should be raised that CLOSE does not say anything about the WFS sensitivity value, which knowledge is of importance for a correct compensation of non-common path aberrations. As a consequence, our present algorithmic design for the SCAO sensor of MICADO includes both CLOSE and a standard algorithm for measuring the WFS optical gain, which seems to be a waste. The possibility of deriving simultaneously an optimum modal gain with the WFS optical gain is currently envisioned, based on the measurements of the correlation for different Δt, possibly leading to an all-in-one algorithm.

ACKNOWLEDGMENTS

The authors express their wishful thanks to D. Montera, whose adaptive control algorithm gave us the push towards designing CLOSE. This research is performed in the frame of the development of MICADO, first light instrument of the ELT (ESO), with the support of ESO, INSU/CNRS and Observatoire de Paris.

REFERENCES

[1] Tamai, R., Cirasuolo, M., González, J. C., Koehler, B., & Tuti, M., "The E-ELT program status," *Proc. SPIE* **9906** (2016).
[2] Liu, F. & Sanders, G., "Thirty meter telescope project status," *Proc. SPIE* **10700** (2018).
[3] Fanson, J., McCarthy, P., Bernstein, R., *et al.*, "Overview and status of the Giant Magellan Telescope project," *Proc. SPIE* **10700** (2018).
[4] Ragazzoni, R., "Pupil plane wavefront sensing with an oscillating prism," *J. Mod. Opt.* **43**(2), 289–293 (1996).
[5] Costa, J. B., "Modulation effect of the atmosphere in a pyramid wave-front sensor," *Appl. Opt.* **44**, 60–66 (2005).
[6] Korkiakoski, V., Vérinaud, C., & Le Louarn, M., "Applying sensitivity compensation for pyramid wavefront sensor in different conditions," *Proc. SPIE* **7015** (2008).
[7] Gendron, É. & Léna, P., "Astronomical adaptive optics. 1: Modal control optimization," *Astronomy & Astrophysics* **291**, 337–347 (1994).
[8] Dessenne, C., Madec, P. Y., & Rousset, G., "Optimization of a predictive controller for closed-loop adaptive optics," *Appl. Opt.* **37**(21), 4623 (1998).
[9] Davies, R., Alves, J., Clénet, Y., *et al.*, "The MICADO first light imager for the ELT: overview, operation, simulation," *Proc. SPIE* **10702**, 107021S (2018).
[10] Clénet, Y., Buey, T., Gendron, É., *et al.*, "The MICADO first-light imager for the ELT: towards the preliminary design review of the MICADO-MAORY SCAO," *Proc. SPIE* **10703**, 10703 – 10703 – 11 (2018).
[11] Deo, V., Gendron, E., Rousset, G., *et al.*, "A telescope-ready approach for modal compensation of pyramid wavefront sensor optical gain," *Astronomy & Astrophysics* **629**, A107 (2019).
[12] Korkiakoski, V., Vérinaud, C., & Le Louarn, M., "Improving the performance of a pyramid wavefront sensor with modal sensitivity compensation," *Appl. Opt.* **47**, 79 (2008).
[13] Montera, D. A., Brown, J. M., Buckman, M. D., *et al.*, "Adaptive gain in closed-loop tilt control and adaptive optics," *Proc. SPIE* **10703**, 10703 – 10703 – 14 (2018).
[14] Deo, V., Gendron, E., Rousset, G., *et al.*, "A modal approach to optical gain compensation for the pyramid wavefront sensor," *Proc. SPIE* **10703** (2018).
[15] Deo, V., *Analysis and implementation of the pyramid wavefront sensor for high-order adaptive optics on ELTs*, PhD thesis, Université de Paris - Observatoire de Paris (2019).
[16] Ferreira, F., Gendron, É., Rousset, G., & Gratadour, D., "Numerical estimation of wavefront error breakdown in adaptive optics," *Astronomy & Astrophysics* **616**, A102 (2018).
[17] Fauvarque, O., Janin-Potiron, P., Correia, C., *et al.*, "Kernel formalism applied to Fourier-based wave front sensing in presence of residual phases," *J. Opt. Soc. Am. A* **36**(7), 1241–1251 (2019).
[18] Chambouleyron, V., Fauvarque, O., Janin-Potiron, P., *et al.*, "Modal gain optimization of the pyramid wave-front sensor using a convolutive model: from theory to experimental validation," in [6^{th} *AO4ELT conference-Adaptive Optics for Extremely Large Telescopes*], (2019).
[19] Conan, J.-M., Rousset, G., & Madec, P.-Y., "Wave-front temporal spectra in high-resolution imaging through turbulence," *J. Opt. Soc. Am. A* **12**(7), 1559 (1995).
[20] Gendron, É., *Optimisation de la commande modale en optique adaptative: applications à l'astronomie*, PhD thesis, Univ. Paris Diderot (1995).
[21] Esposito, S., Pinna, E., Puglisi, A., *et al.*, "Non common path aberration correction with non linear WFSs," in [4^{th} *AO4ELT conference-Adaptive Optics for Extremely Large Telescopes*], (2015).
[22] Vidal, F., Ferreira, F., Deo, V., *et al.*, "Analysis of the MICADO-MAORY SCAO performance," in [6^{th} *AO4ELT conference-Adaptive Optics for Extremely Large Telescopes*], (2019).
[23] Gratadour, D., Ferreira, F., Sevin, A., *et al.*, "COMPASS: status update and long term development plan," *Proc. SPIE* **9909** (2016).
[24] (a): www.tinyurl.com/singleStarCLOSE; (b): www.tinyurl.com/doubleStarCLOSE; (c): www.tinyurl.com/TitanCLOSE.
[25] Guyon, O., "Limits of adaptive optics for high-contrast imaging," *Astrophysical Journal* **629**(1) (2005).
[26] Clergeon, C., *Étude d'un analyseur de surface d'onde haute sensibilité pour l'optique adaptative extrême*, PhD thesis, Observatoire de Paris - Subaru National Astronomical Observatory of Japan (2014).
[27] Deo, V., Gendron, E., Rousset, G., *et al.*, "Assessing and mitigating alignment defects of the pyramid wavefront sensor: a translation insensitive control method," *Astronomy & Astrophysics* **619**, A56 (2018).